# A Study of Gain Tuning for Prolonged Physical Contact of Fully-Actuated UAVs

Chantelle Singh, Shahab Kazemi, Jonty Kirk, Katrina Chan, and Karl Stol
Department of Mechanical and Mechatronics, University of Auckland, New Zealand.
Corresponding author Email: shahab.kazemi@auckland.ac.nz

## ABSTRACT

This study explores achieving stable, prolonged physical contact with a fully-actuated multi-rotor unmanned aerial vehicle (UAV). Through rigorous experiments, we analyze the dynamic interplay between an octocopter UAV and its environment, particularly concerning the influence of control gains on system behaviour. Employing the widely-used P-PID controller, the paper unravels the implications of vibrations and instabilities during UAV operation. Using five different angles, the research elucidates how tuning P-PID gains based on contact angle and dynamic coupling impacts the UAV's response to external forces, enhancing stability and overall performance. Moreover, the effect of the center of mass (CoM) location is also considered a factor affecting the experiments. The results show that the response of the UAV after tuning is capable of robust contact testing.

http://www.imavs.org/

## 1 INTRODUCTION

Unmanned aerial vehicles (UAVs) applications include but are not limited to surveying, mapping, inspecting, plant and wildlife preservation, agriculture, and atmospheric science monitoring, as detailed in various studies [1, 2, 3, 4, 5]. In this context, emerging technologies have made it inevitable for UAVs to demonstrate robust performance and stability in executing physical interactions, such as grasping, sampling, contact-based inspecting, transporting, and assembling. A UAV application involves two-way physical interaction, where the UAV applies force and receives reactions from its surroundings. These interactions can significantly affect the UAV's behavior.

UAVs conducting physical interaction is called aerial manipulation, which is manipulating the environment in mid-air. Aerial manipulation is of recent interest due to the several applications it is suited to. Some examples of aerial manipulation applications are shown in Figure 1.

There are many interesting studies related to UAVs' physical interactions. A study introduced and validated an armed-UAV for valve manipulation. Using a human-machine interface, a single operator directed the UAV to approach, grasp, and rotate an industrial valve using arm motion and voice control. The system demonstrated exceptional stability and resilience to contact forces [6]. In another study a 6-m-tall tower of 1500 foam modules was constructed in 18 hours using four autonomous quadcopters [7]. For precise aerial repair, explicitly focusing on sealing and filling cracks, an integrated 3-degrees of freedom (-DoF) manipulator capable of compensating for both translational and rotational offsets attached to the UAV frame was proposed. The outcomes highlighted potential applications for accurate aerial inspections and repairs in demanding environments, such as nuclear or petrochemical plants [8]. The UAVs interactions with trees for canopy sampling were discussed in [9]. The sampling procedure was segmented into four phases: unimpeded flight to reach the branch, actively tracking the branch's position, coupling and decoupling from the branch, and finally, departing from the canopy. An octocopter configuration incorporated a novel manipulator, enabling robust contact operations for precise inspections [10]. The manipulator, rotating around the UAV's CoM, oriented the end effector within 180 degrees of the workspace, efficiently rejected external perturbations, maintained a specific contact force against the surface, and calculated the end effector's position concerning the aerial robot.

Another application is the use of UAVs for inspecting infrastructure, specifically power transmission assets, which has garnered significant attention due to its potential to improve safety and cost-effectiveness in the energy transmission sector [1]. Powerline contact testing is preferable to non-contact testing as quantitative information such as voltage drop, current, and resistance can be found by physically testing the powerline using a probe[1] (visual power line testing can use thermal imaging to detect overheating conductors and regular imaging to detect potential structural damage to cables). Ikeda et al. researched the flight control of an under-actuated UAV contact testing a bridge with a single DoF manipulator [11]. The manipulator used was a rigid connection extended horizontally from the UAV. The UAV tested the bridge for structural faults by sending ultrasonic pulses through the structure.

Similar to the powerline contact testing, there are certain forces that the controller has to deal with. Through experimental analysis, it was observed that the pitch angle of the UAV during contact with the bridge wall is closely correlated

[1] https://www.scribd.com/document/428682812/SensorLink-Catalogue-pdf

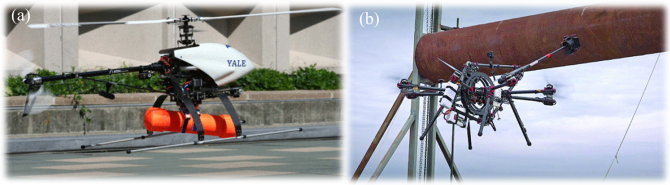


Figure 1: Aerial manipulation examples. (a) Helicopter carrying an object [13]. (b) UAV with manipulator for inspection at industrial sites [10]

with the corresponding contact force experienced by the UAV. They used classical control in the form of cascaded proportional, integral, and derivative (PID) control to keep the UAV stable while it was in contact with the bridge. When UAVs deliberately interact with the environment, the standard position control architecture for a free-flying UAV is no longer robust. Tomic and Haddadin [12] considered this control problem in creating a unified framework for UAV interaction control. They proposed using admittance and impedance controllers in developing control for UAVs to allow for compliance with obstacles allowing for less rigid contact.

This study aims to achieve stable contact testing with a fully-actuated UAV and a rigidly attached arm by systematically tuning the free-flight gains based on different angles through which it made the physical contact. The fully-actuated UAV can perform pure translation without having to tilt (translating and maintaining flight stability without having to pitch or roll) while providing a horizontal thrust. The ability to exert force without titling makes the fully-actuated UAV suitable for rigid arm attachments. The rest of this article is organized as follows.

In Section 2, we detail the physical setup, including the fully-actuated UAV configuration and specific contact attachments, establishing a foundation for the experimental context. Additionally, Section 2 dives into software and hardware integrations, ensuring the readiness of the setup. Section 3 shifts focus to the control structure, explaining the difference between the used controller and the standard PX4 algorithm. Section 4 presents gains tuning tailored for experimental scenarios, results, detailing the UAV's performance during prolonged physical interactions and responses to varied contact angles. The accompanying analysis provides deeper insights. Section 5 concludes with a concise summary of contributions and outlines potential future research directions.

## 2 UAV AND EXPERIMENTAL SETUP DESCRIPTION

The fully-actuated UAV used in this paper is an octocopter consisting of four rotors on the top and four rotors on the bottom (see Figure 2). Each of these rotors is fixed at 31º, allowing for translation in the X and Y directions without pitching or rolling (flying level). This characteristic is essential because the physical interaction mechanism consists of an arm and end effector (inspired by the prob from SensorLink[2]) rigidly attached to the UAV at specific angles, requiring the UAV to fly level when making contact with its surroundings. As the external environment, a long horizontal clamped-clamped rod with a stiffness of 508 N/m a is used (0.5 m above the ground). During each experiment, the UAV must exert a force on the rod while remaining level to ensure that it applies the force at a specific angle (0º, 45º, 90º, -45º, or -90º). If the UAV changes its attitude such that it no longer has minimal roll and pitch, it is challenging to get stable contact with sufficient force being applied by the UAV as it will slip or flip around the rod. In order to create a rigid attachment between the arm and the UAV, a C-shaped rig is designed (laser cut out of a 6 mm acrylic sheet), allowing for securing a carbon fiber arm (low weight and high strength) to the airframe by five different angles in a vertical body-fixed plane shown in Figure 3. The C-shaped rig is placed in a way that has no interference with the propellers, allowing for a safe flight. The rig is firmly attached at all points with additional mounting brackets to ensure rigid connections and less vibration.

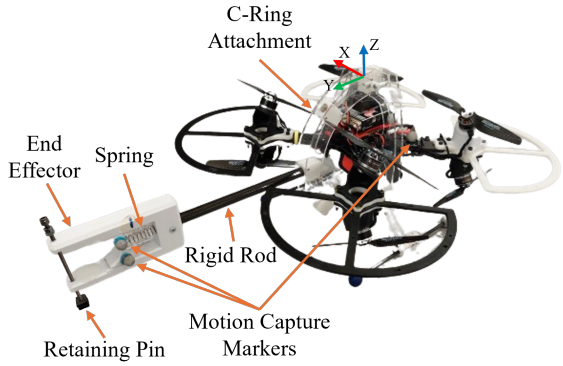


Figure 2: Fully-actuated octocopter used. X, Y, Z are body frame coordinates

In this paper the end effector, including the attached carbon fibre rod, has a total mass of 43 g. A safety retaining pin, which has minimal effect on the experimental results, is added as a precaution in case something goes wrong. In addition, a spring is embedded into the end effector to determine the contact force by measuring its compression. Figure 4 shows the calibration result using an analogue force gauge to find the relationship between the force and displacement of the spring. The spring's displacement is readily measurable by adding two reflective markers and using the motion capture system. The approach provides a straightforward method to calculate the force exerted from the end effector to the clamped rod instead of force sensors, which may add significant complexity due to increased weight, communica-

[2]https://www.scribd.com/document/428682812/SensorLink-Catalogue-pdf

http://www.imavs.org/

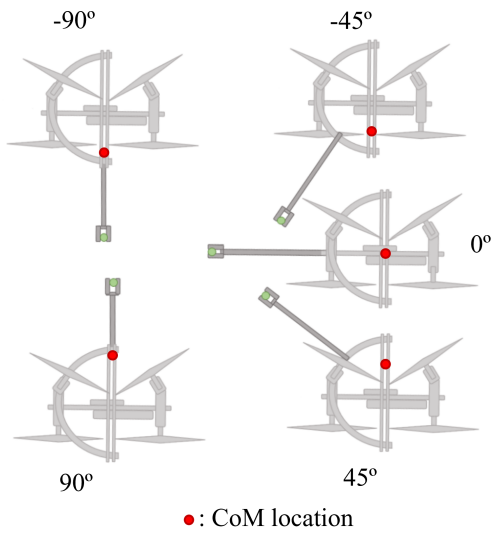


Figure 3: Contact angles showing CoM location

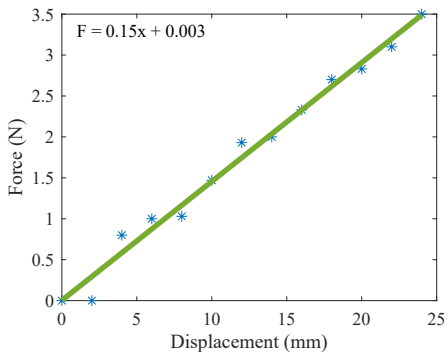


Figure 4: Calibration graph for the end effector's spring, based on data captured from bench handheld experiments

tion challenges, and integration with the flight controller. Due to all the mentioned physical modifications, the mass of the UAV is increased from 806 g to 977 g.

Since this research only focuses on physical interaction, as opposed to tracking a trajectory and making physical contact, a safety retaining pin and tether is be used during the experiment. The tether was attached around the top of the UAV and set up to be extremely loose. Note that the impacts of these safety features are minimal and only in effect during arming and disarming portions of the flight and not during contact.

All the experiments are conducted in a motion capture laboratory consisting of several cameras to track the movement of reflective markers attached to specific parts of the UAV. Also, a Simulink platform is used to send the setpoints required by the offboard controller to the UAV. The offboard controller is a position controller that can send position and attitude setpoints to the UAV. The controller is uploaded on the Pixhawk 4 Mini flight controller (attached to the UAV), which uses an ESP32 microcontroller to communicate with an offboard computer using the MAVLink protocol. Figure 5 shows the relationships between the hardware elements of the experiment.

After turning on the motion capture system, the PC used for generating the set points is connected to the UAV Wi-Fi module and then runs the Simulink interface. In the next step, the motion capture readings must correlate with the sensor readings from the Pixhawk 4 on the UAV through the EKF2 module. After ensuring that the motion capture data matches the onboard Pixhawk 4 sensors, the UAV manually takes off using the transmitter. Immediately after the take-off, the pilot switches to the offboard controller to start regulating toward the desired setpoints. The setpoint regulation is executed through the Simulink interface, sending high-level setpoints for position. Note that the desired set points, which are the position of the UAV relative to the contact point, are determined previously using motion capture markers by placing the unarmed UAV in the required location for contact and analysing the vicon tracker readings. After finishing the prolonged contact, the human pilot disarms the UAV. The last step involves collecting the flight log and motion capture recording data, which is then used to calculate the displacement of the spring on the end effector to calculate the coaxial compression force. This procedure is shown as a flowchart in Figure 6.

## 3 CONTROL STRUCTURE

The utilized controller is a customized iteration of the standard P-PID controller integrated with the PX4 Autopilot version 1.12.3[3]. The standard P-PID involves a PID attitude rate controller, the innermost control loop, and a P controller for attitude (Euler angles). Additionally, we have the velocity PID controller and the position P controller. In this paper, we focus on the position and velocity of P-PID loops. In standard PX4 Autopilot, the translational commands from position control are converted to angle setpoints and passed to the attitude controller (in a cascaded form). In this work, however, the attitude controller runs parallel to the position controller, with constant zero setpoints for angles to keep the UAV level during the flight. Figure 7 shows the block diagram of the used controller.

As mentioned before, the focus of this work is exploring the P-PID gains and their effect on the physical interaction mission. A systematic approach to modifying the controller gains is taken by initially tuning the control gains for free flight. To begin this process, the attitude rate controller is tuned first since it is more sensitive. Tuning involves flight tests after incremental gain changes and response analyses. Once the rate controller is tuned with acceptable root mean square error (RMSE) values, the attitude, velocity, and position controllers are tuned. These free flight gains provide the

[3]https://docs.px4.io/v1.12/en/

http://www.imavs.org/

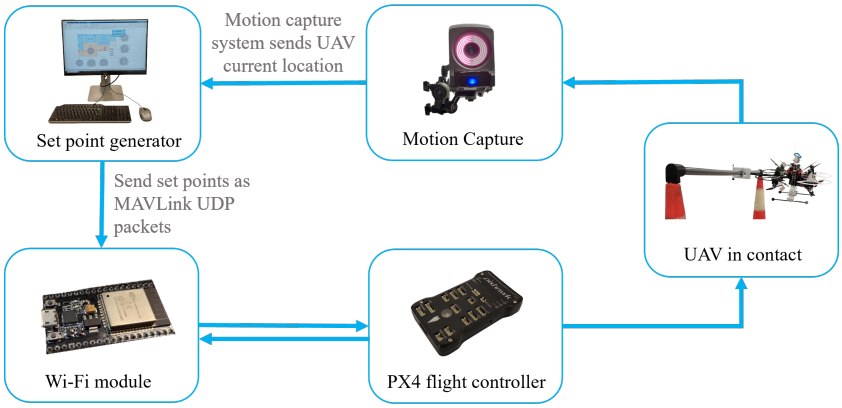


Figure 5: Connection between different parts of the experimental setup

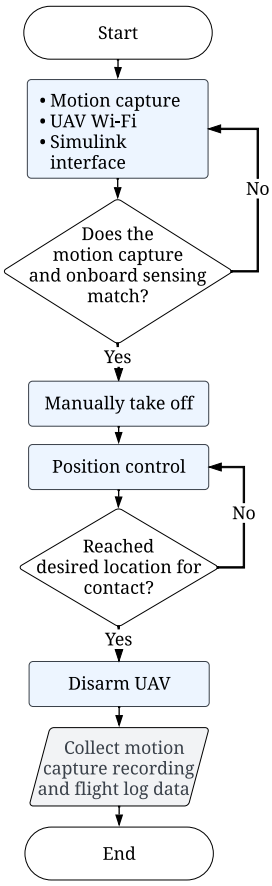


Figure 6: Experimental Process

base gains used in the first in-contact flight experiments with different contact angles.

## 4 EXPERIMENTAL GAIN TUNING

Table 1 shows the physical contact requirements including the time, force and different angles. Most research studies in UAV contact testing hold contact for 10 seconds [11, 14]. This study initially chose to use 10 seconds; however, it decided to increase this to 30 seconds to showcase the ability of the UAV to sustain prolonged contact. The contact force requirements is 1N or more, which is the 50% of the maximum horizontal force in hover by the utilized UAV in [15]. This force is suitable, as it is within the safe limits of motor saturation for this UAV. Five different angles are chosen to represent a successful and prolonged physical interaction. These angles are chosen, as previous research on contact-based inspection UAVs have decided on these angles as suitable angles required for contact based inspection applications [16]. For each angle there is a coupling between different DoF that conflict. Coupling is when the motion in a certain DoF is linked with the motion in another DoF. Therefore, when the UAV translates or rotates in one DoF, the motion of the other DoF will be affected. This can lead to issues such as a large accumulation of errors in different DoFs. This results in issues such as extreme vibrations, saturation, and instability. Although the UAV is balanced horizontally, due to the end effector attachment, the CoM is slightly above or below the original CoM location. The motor mixer designed and implemented in the firmware for this UAV is optimized for the CoM being precisely in the centre of the UAV. Adding an end effector in angles higher or lower results in the CoM moving. Therefore, due to this, there is an undesired torque affecting the resulting contact for certain angles. In order to eliminate coupling effects, the P-PID gains discussed in Section 3 will be experimented. Although a thorough investigation of gain tuning was conducted with the experimentation of different gain magnitudes and combinations, the minimal amount of change required for successful contact is chosen for the fi-

http://www.imavs.org/

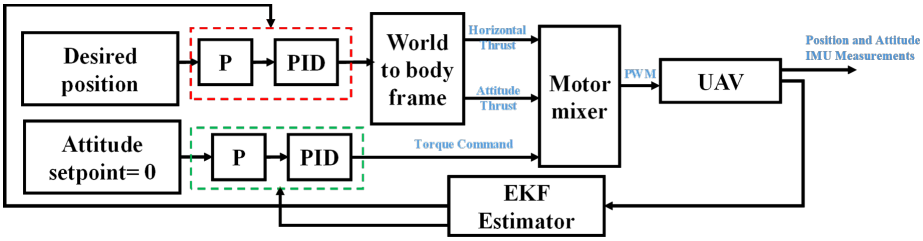


Figure 7: PX4 P-PID Control Architecture

| Requirement | Value |
|---|---|
| Angle selection (deg) | 0, 45, 90, -45, -90 |
| Force (N) | $\geq 1$ |
| Contact time (s) | $\geq 30$ |

Table 1: Contact testing requirements

nal experiments. Figure 8 shows all the successful prolonged interaction experiments with different angles[4]. In the following, the gain tuning logic based on the angles and position of CoM are discussed thoroughly:

### 4.1 0º contact angle

The experiment begins with the end effector and arm inserted into the 0º angle. The first step in this process is to test the 0º angle with the free flight gains. This is to compare later with experiments with modified gains. The 0º contact angle free flight experiments show relatively stable results. Following this, the second experiment repeated the 0º test with gains designed to eliminate coupling effects. For this particular angle, there is a coupling between the X-axis (sideways) and yaw (the axes are shown in Figure 2). There is also a coupling between the Z-axis and the pitch-axis. These couplings have the potential to cause large errors in different axis due to conflicting motions. For example, when the UAV increases in height, if it strays away from the setpoint, it inevitably causes a rotation around the pitch axis, leading to significant pitch errors, integral wind-ups and flips around the pitch axis. Additionally, there is also vibration due to this. Several experiments involve zeroing the axis where less precision is needed for contact for each coupling. Yaw and pitch were zeroed resultantly. These essentially reduce the system's motion from 6 DoF to 4 DoF since there is no longer any control over the pitch and yaw axis. However, for this contact angle, a positive result is seen for either free flight or the modified gains. Vibration is present but not as significant as in other angles, elaborated more below.

### 4.2 -45º contact angle

Like with the 0º contact angle, it is suspected that coupling would interfere with contact testing at a contact angle of -45º angle, pitch is coupled with Y-axis and Z-axis. Pitch gains are to be zeroed to test if eliminating the coupling will improve contact testing. However, this leads to an unstable flight with large oscillations in the pitch. The free flight gains are better suited to this contact angle over zeroing pitch gains. This is due to the overall UAV CoM being below the original UAV CoM, which is slightly below the mid plane of the stacked rotors due to the end effector weight. This leads to undesired moments, which causes the pitch axis instability; hence, free flight gains are ideal for this contact angle. Although, with free flight gains, there are some minimal vibrations in the pitch axis (due to issues such as coupling between the pitch, Y, and Z axis), it is not significant to prevent stable contact.

### 4.3 -90º contact angle

Similarly to the 0º angle, it was hypothesized that coupling between axes prevents free flight gains for a stable physical interaction. However, for the -90º contact angle, the axis coupled are different. Here, the pitch is coupled with the Y-axis, and the roll is coupled with the X-axis. Since the X and Y gains are one gain in PX4, pitch gains are zeroed. Like the -45º contact angle, the CoM is below the UAV's original CoM that the motor mixer was created for. Therefore, the undesired moments caused similar oscillations that are observed for -45º. Subsequently, free flight gains result in stable contact with minimal vibrations.

### 4.4 +45º contact angle

Coupling for this angle is the same as the -45º angle, where the pitch is coupled with the Y and Z axes. However, due to the end effector being angled upwards, the CoM is above the expected location for which the motor mixer was designed. Experiments show that this contact angle is stable with the pitch gains zeroed. Free flight gains will not work for this angle as significant vibration is observed, leading to saturation. Contact is impossible due to the saturation preventing the UAV from applying forces via the end effector on the flexible rod for contact. Further tests demonstrated that only zeroing the pitch gains prevented vibration and saturation issues.

### 4.5 +90º contact angle

Having a similar coupling with the -90º contact angle, the only reason that makes the gains required different is the lo-

[4]https://youtu.be/4GtdBr-9Ae8

http://www.imavs.org/

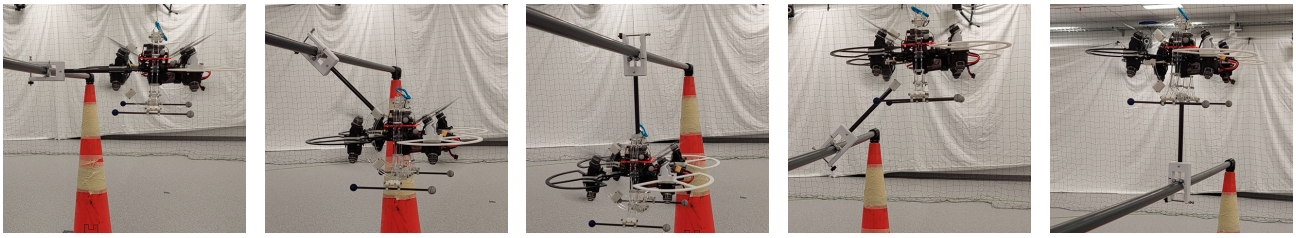

(a) 0º (b) 45º (c) 90º (d) -45º (e) -90º

Figure 8: Contact testing for each angle

cation of the COM. Here, the COM is above what the motor mixer expects during experiments, zeroing the pitch gains results in stable flight without any instability observed. This also eliminates excessive vibrations observed with free flight gains.

The above experimental process is repeated several times to validate the results. It is discovered that the pitch axis coupling is the leading cause of vibration and saturation of some rotors. The UAV becomes stable by zeroing the most negative coupling observed in experiments, which is due to the pitch axis, where the UAV tends to vibrate in this axis significantly for certain angles, depending on the position of the CoM. Horizontally, the UAV can always be balanced by shifting the battery back or forth. However, it is difficult to keep the CoM vertically in the UAV's centre if the arm is at angles other than 0º. Table 2 shows the experimental results in a meaningful order. It is observed that if the CoM is above the UAV's central horizontal plane, the pitch gains must be zeroed to avoid vibration from the coupling effect. On the contrary, if the CoM is below the UAV's central horizontal plane, we need to keep the free flight gains, including the pitch gains, as they are to avoid creating an unwanted moment. After tuning the gains, the UAV shows stability such that the overall roll, pitch, and yaw angles remain small. (see Table 3). It can be seen that the UAV is relatively stable with roll, pitch, and yaw varying from the setpoint within $\mp 6$º as shown in Figure 9. The compression force for the -45º contact angle is shown in Figure 9a showing the consistent force above 1N for a 30 s time period. Additionally, the attitude over the compression period for this angle are shown in Figure 9b. The mean electrical power values in Table 3 are similar across different angles for comparable compression forces, reflecting the energy required to maintain stable contact. This results from tuning the gains to combat issues such as vibration due to coupling or instability. Before tuning, different DoF are coupled, affecting the contact and requiring a much larger power to make contact with the same force. Table 4 shows that the fully-actuated UAV can successfully maintain a leveled physical contact, which is essential as the arm is rigidly attached to the UAV at a certain angle. The only exception is the 45º contact angle, which has a noticeably larger pitch RMSE of 9.3º, although the response is still stable and meets the time and force requirements.

| Angle (deg) | CoM location | Gains |
|---|---|---|
| 0 | Center | Free flight/Zero pitch |
| 45 | Above | Zero pitch |
| 90 | Above | Zero pitch |
| -45 | Below | Free flight |
| -90 | Below | Free flight |

Table 2: Gains required for stable contact

| Angle (deg) | Mean force (N) | Mean electrical power (W) |
|---|---|---|
| 0 | 2.19 | 246 |
| 45 | 2.87 | 396 |
| 90 | 2.42 | 342 |
| -45 | 2.90 | 250 |
| -90 | 2.54 | 269 |

Table 3: Contact testing power and force analysis over 30 second compression period

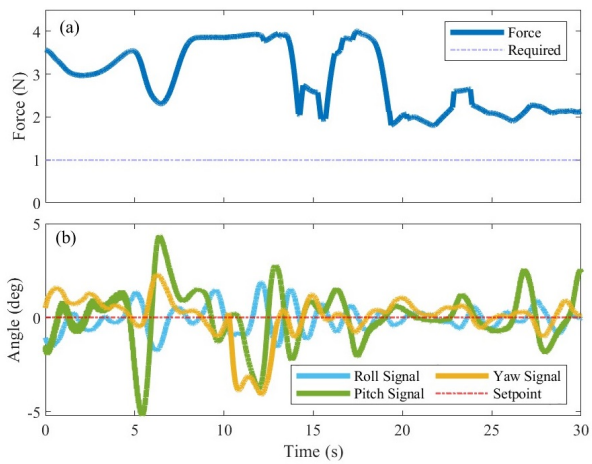


Figure 9: a) Force compression during -45º contact angle. b) Attitude (Euler angles) during physical interaction for -45º

http://www.imavs.org/

| Angle (deg) | Roll (deg) | Pitch (deg) | Yaw (deg) |
|---|---|---|---|
| 0 | 0.1 | 1.4 | 0.7 |
| 45 | 0.2 | 9.3 | 0.6 |
| 90 | 1.6 | 0.8 | 0.3 |
| -45 | 0.7 | 1.5 | 1.2 |
| -90 | 1.2 | 0.4 | 0.3 |

Table 4: RMSE over 30 seconds compression period

## 5 CONCLUSION

In conclusion, this study delved into the impact of coupling-dependent gain tuning on the prolonged physical interaction of a fully-actuated UAV. Through extensive testing involving five different contact angles for prolonged contact experiments, it became evident that coupling between degrees of freedom can impede sustained contact. The placement of the arm also influences the CoM, introducing complexities, notably when the CoM deviates from the expected 2D plane specified by the motor mixer. This deviation, significantly above the expected plane, results in significant oscillations along the pitch axis, necessitating the zeroing of pitch gains for stability. The study highlights the need for further exploration, suggesting a natural progression to achieve contact tests from free flight gains, flying towards the rod, and switching gains at the point of contact. Exploring different controllers for contact testing across various angles could enhance results. Moreover, research into the potential mid-flight rotation of the manipulator's arm would allow the UAV to take off and rotate the arm to an angle that the UAV cannot take off, e.g., 90º. This would have promising avenues for improved efficiency and versatility in UAV operations.

## ACKNOWLEDGMENT

The research reported in this article was conducted as part of "Enabling unmanned aerial vehicles (UAVs) to use tools in complex dynamic environments "UOCX2104", which is funded by the New Zealand Ministry of Business, Innovation and Employment.

## REFERENCES

[1] Ryan Kitchen, Nick Bierwolf, Sean Harbertson, Brage Platt, Dean Owen, Klaus Griessmann, and Mark A Minor. Design and evaluation of a perching hexacopter drone for energy harvesting from power lines. In *2020 IEEE/RSJ International Conference on Intelligent Robots and Systems (IROS)*, pages 1192–1198. IEEE, 2020.

[2] Youngjib Ham, Kevin K Han, Jacob J Lin, and Mani Golparvar-Fard. Visual monitoring of civil infrastructure systems via camera-equipped unmanned aerial vehicles (uavs): a review of related works. *Visualization in Engineering*, 4(1):1–8, 2016.

[3] Julie Linchant, Jonathan Lisein, Jean Semeki, Philippe Lejeune, and Cédric Vermeulen. Are unmanned aircraft systems (uas s) the future of wildlife monitoring? a review of accomplishments and challenges. *Mammal Review*, 45(4):239–252, 2015.

[4] Guangying Jiang, Richard M Voyles, and Jae Jung Choi. Precision fully-actuated uav for visual and physical inspection of structures for nuclear decommissioning and search and rescue. In *2018 IEEE international symposium on safety, security, and rescue robotics (SSRR)*, pages 1–7. IEEE, 2018.

[5] Tzu-Jui Lin and Karl A Stol. Towards automated under-canopy exploration of plantation forests. In *2019 International Conference on Unmanned Aircraft Systems (ICUAS)*, pages 1201–1208. IEEE, 2019.

[6] Matko Orsag, Christopher Korpela, Stjepan Bogdan, and Paul Oh. Valve turning using a dual-arm aerial manipulator. In *2014 international conference on unmanned aircraft systems (ICUAS)*, pages 836–841. IEEE, 2014.

[7] Frederico Augugliaro, Sergei Lupashin, Michael Hamer, Cason Male, Markus Hehn, Mark W Mueller, Jan Sebastian Willmann, Fabio Gramazio, Matthias Kohler, and Raffaello D'Andrea. The flight assembled architecture installation: Cooperative construction with flying machines. *IEEE Control Systems Magazine*, 34(4):46–64, 2014.

[8] Pisak Chermprayong, Ketao Zhang, Feng Xiao, and Mirko Kovac. An integrated delta manipulator for aerial repair: A new aerial robotic system. *IEEE Robotics & Automation Magazine*, 26(1):54–66, 2019.

[9] James R Kutia, Karl A Stol, and Weiliang Xu. Aerial manipulator interactions with trees for canopy sampling. *IEEE/ASME transactions on mechatronics*, 23(4):1740–1749, 2018.

[10] Anibal Ollero, Guillermo Heredia, Antonio Franchi, Gianluca Antonelli, Konstantin Kondak, Alberto Sanfeliu, Antidio Viguria, J Ramiro Martinez-de Dios, Francesco Pierri, Juan Cortés, et al. The aeroarms project: Aerial robots with advanced manipulation capabilities for inspection and maintenance. *IEEE Robotics & Automation Magazine*, 25(4):12–23, 2018.

[11] Takahiro Ikeda, Shogo Yasui, Motoharu Fujihara, Kenichi Ohara, Satoshi Ashizawa, Akihiko Ichikawa, Akihisa Okino, Takeo Oomichi, and Toshio Fukuda. Wall contact by octo-rotor uav with one dof manipulator for bridge inspection. In *2017 IEEE/RSJ International Conference on Intelligent Robots and Systems (IROS)*, pages 5122–5127. IEEE, 2017.

http://www.imavs.org/

[12] Teodor Tomić and Sami Haddadin. A unified framework for external wrench estimation, interaction control and collision reflexes for flying robots. In *2014 IEEE/RSJ international conference on intelligent robots and systems*, pages 4197–4204. IEEE, 2014.

[13] Paul E. I. Pounds, Daniel R. Bersak, and Aaron M. Dollar. Grasping from the air: Hovering capture and load stability. In *2011 IEEE International Conference on Robotics and Automation*, pages 2491–2498, 2011.

[14] Karen Bodie, Maximilian Brunner, Michael Pantic, Stefan Walser, Patrick Pfändler, Ueli Angst, Roland Siegwart, and Juan Nieto. Active interaction force control for contact-based inspection with a fully actuated aerial vehicle. *IEEE Transactions on Robotics*, 37(3):709–722, 2021.

[15] Pedro Henrique Mendes Souza. *Dynamics and Control of Unmanned Aerial Vehicles for Prolonged Interaction with Compliant Environments*. PhD thesis, ResearchSpace@ Auckland, 2023.

[16] Robert Watson. *Unmanned Aerial Vehicles for Contact-Based Inspection*. PhD thesis, University of Strathclyde, 2023.

http://www.imavs.org/